Effect of Electrolyte Concentration on the Dynamic Surface Tension and Dilational Viscoelasticity of Adsorption Layers of Chitosan and Dodecyl Chitosan

Valery G. Babak,* Rachel Auzely, and Marguerite Rinaudo

Centre de Recherches sur les Macromolécules Végétales, CNRS, Laboratoire Associé à l'Université Joseph Fourier, BP53- 38041 Grenoble cedex 9, France

Received: March 7, 2007; In Final Form: June 12, 2007

The effect of an external salt (AcONa) on the kinetics of adsorption and structure formation inside the adsorption layers (ALs) of chitosan (Ch) and dodecyl chitosan (C_{12}Ch) as well as on the frequency dependence of the complex dilational elasticity modulus of these layers has been studied. The complex dilational elasticity modulus of adsorption layers of polymers has been measured on the drop tensiometer (Tracker, IT Concept, France) upon applying a small sinusoidal variation of the drop area with a given frequency, ω, in the range from 10^{-2} to 0.63 rad/s and recording the variation of the surface pressure. It has been found that, in the absence of the salt, the dilational storage modulus, $E'(\omega)$, of ALs of both Ch and C_{12}Ch is lower with regard to the loss modulus, $E''(\omega)$, in the whole range of frequencies used, testifying for the liquidlike rheological behavior of these layers. With an increase of the salt concentration up to $C_{AcONa} > 0.1$ M, the ALs become solidlike, as shown when $E'(\omega) > E''(\omega)$. Consequently, the characteristic frequency, ω_c, corresponding to the intercept between the $E'(\omega)$ and $E''(\omega)$ curves, gradually varies from $\omega_c > 1$ rad/s to $\omega_c < 0.01$ rad/s when the salt concentration is increased from zero to $C_{AcONa} = 1$ M. Hydrophobically modified C_{12}Ch, having long grafted alkyl chains, exhibited a higher sensitivity to the presence of salt than Ch: the former solidifies more readily and at lower salt concentrations than the latter. It has been found that the experimental $E'(\omega)$ and $E''(\omega)$ curves exhibit two characteristic relaxation frequencies, $\omega_{01} \sim 1$ rad/s and $\omega_{02} \sim 10^{-3}-10^{-2}$ rad/s, whose physical meaning and values were related to the structure of the ALs and to the competitive contribution of electrostatic and hydrophobic interactions between amino and nonpolar groups of Ch and C_{12}Ch to the formation of a gel-like network inside the polymeric film at the interface.

Introduction

Hydrophobic modification of polyelectrolytes (PEs) by covalent binding of a small quantity (few mol %) of long alkyl chains does not significantly decrease the solubility of these PEs in water but makes them very surface active and able to form intra- and inter-macromolecular associates (aggregates) via hydrophobic interaction between alkyl chains.[1−4] The driving force of these spontaneous adsorption and self-association (aggregation) phenomena is a considerable gain in free energy ($\sim$10 kT[5]) when relatively long grafted alkyl, e.g., dodecyl, chains are transferred from water to a nonpolar (air or oil) phase or inside a hydrophobic core of micelle-like aggregates. With an increase in the hydrophobe content in the PE (the alkyl chain length and/or the degree of alkylation), this tendency to adsorption and self-association increases (in the limits of the PE solubility), although the additivity principle is not always observed.[6] Other factors such as flexibility of the macroion backbone affected by the presence of salt and the hydrophobicity of repeated units could play a remarkable role in these properties.[2,6]

In the case of a cationic polyelectrolyte, chitosan (Ch), which is insoluble at normal pH but soluble at acidic pH due to protonation of the NH_2 groups of the D-glucosamine units, the hydrophobicity of the −CH groups and of the −N-acetyl groups of the N-acetyl D-glucosamine units is responsible for relatively low but remarkable surface activity (the ability to decrease the interfacial tension)[6−8] and the ability to form hydrophobic aggregates in the aqueous solutions.[9] Although the gain in the free energy resulting from adsorption of these small hydrophobic groups is of the order of 1 kT, the adsorption of the chitosan having relatively high molecular mass (>100 kDa) is irreversible,[10] as explained by the multiplicity of these hydrophobic units. On the other hand, the hydrophobically modified chitosan (HMCh) containing long alkyl chains covalently grafted[11,12] adsorbs irreversibly at the interfaces.[6,13] At the same time, with decreasing molecular weight down to 5 kDa, both Ch and HMCh exhibit reversible adsorption even with the degree of alkylation achieving $\sim$10 mol %.[14]

At relatively low bulk concentrations, the HMCh manifests, like proteins,[15−17] three characteristic stages of adsorption: lag stage, post-lag stage, and final stage. The first two stages correspond to relatively loose packing of macromolecules at the interface relating to gaseous and liquid extended states of the adsorption layer. These stages are characterized by low lateral intermolecular interaction between adsorbed macroions and electrostatic interaction between protonated $-NH_2$ functional groups.[13,18]

The last stage is characterized by intensive steric, hydrophobic, and electrostatic interactions between laterally compressed macroions. During this stage, one observes a sharp increase of the two-dimensional total elasticity modulus, E, of the adsorption layers measured by dynamic dilational rheometry[6,19] at some relatively high circular frequency, $\omega \sim 1$ rad s^{-1}.[13,20] The

* Corresponding author. Present address: 28, Vavilova str., Moscow 117813, Russian Federation. Phone: +7-495-1356502. Fax: +7-495-1355085. E-mail: babak@ineos.ac.ru.

10.1021/jp0718653 CCC: $37.00
Published on Web 07/21/2007

increase of E was attributed to numerous cross-links formed by the associating hydrophobic units (between alkyl chains and other hydrophobic moieties) of neighboring adsorbed macroions, leading to the formation of a physical gel-like structure inside the adsorption layers. It has been observed[20] that, at this frequency, the adsorption layers of HMCh having 5 mol % grafted C_{12} groups and formed at 0.18 g/L solution in the 0.3 M AcOH/0.0.5 M AcONa buffer behave as solidlike while the dilational storage modulus, E', is higher than the loss modulus, E''. Under the same conditions, the adsorption layers of Ch behaved as liquidlike, satisfying the inequality $E' < E''$.

The frequency variations of $E'(\omega)$ and $E''(\omega)$ for these PEs in the range $\omega = 0.03-0.3$ rad/s are not purely Maxwell, which is ascertained by more or less considerable deviation of these moduli from the scaling laws $\omega/(1 + \omega^2)$ and $\omega^2/(1 + \omega^2)$, respectively.[13,20] This testifies for multiple relaxation processes in the adsorption layers occurring with different characteristic relaxation times.[21] It has been found that the crossing frequencies, ω_c, at which the curves $E'(\omega)$ and $E''(\omega)$ intercept each other, are drastically different for Ch and HMCh: the former has $\omega_c \sim 0.1-1$ rad s^{-1}, whereas the latter has $\omega_c \sim 10^{-3}-10^{-2}$ rad s^{-1}.[13,20]

It has been found that this crossing frequency, ω_c, is very sensitive to the variation of the physicochemical factors such as bulk concentration, C_p, of PE,[20,21] complex formation with oppositely charged surfactants (SDS)[6,20,22] or polyelectrolytes (chitosan sulfate),[10] etc. The increasing C_p makes the adsorption layers more liquidlike; for example, for HMCh having 5 mol % dodecyl groups, the crossing frequency, ω_c, increased exponentially from 0.03 to 0.3 rad/s when C_p increased from 0.003 to 0.75 g/L.[13,21] This result proves that the adsorption−desorption rate of alkyl chains of the macroions localized in the vicinity of the interface (inside a nearest subphase layer) plays a remarkable role in the relaxation phenomena: the higher the concentration of these chains, the faster the rate of their adsorption by diffusion, and the smaller the relaxation time.[21] Adding SDS to Ch solution produces solidification of the adsorption layers; for example, the crossing frequency, ω_c, decreased from 1.3 to 0.03 rad s^{-1} when the relative SDS concentration in the SDS−Ch solution increased from zero to $C_{SDS} \sim 2$ mol %.[21] A more spectacular decrease of the crossing frequency, ω_c, from ~1 to $<10^{-3}$ rad s^{-1} has been recorded in the course of the formation of the interfacial inter-polyelectrolyte complexes between the Ch and the chitosan sulfate.[10,22]

Practically no attention has been drawn to the effect of the salt on the viscoelastic properties of adsorption layers of Ch and HMCh, and, in general, to the adsorption layers of associating polyelectrolytes. In the meantime, according to concepts and views developed and formulated in refs 23 and 24, the viscoelastic and other physical properties of aqueous solutions and adsorption layers of these PEs result from a balance of electrostatic repulsions and hydrophobic attractions controlled by the screening effect of external salts. Recently, it has been shown that salt exerts a strong effect on the viscoelastic properties of aqueous solutions of HMCh by decreasing the crossing frequency.[25] In this connection, it will be interesting to compare this effect with the effect of the salt on the viscoelasticity of the adsorption layer of Ch and HMCh at the air/acidic aqueous solution interface.

In this paper, the objective was to study the effect of the external salt concentration on the adsorption and structure formation kinetics inside the adsorption layers of chitosan and C_{12} alkyl chitosan (during the aging time up to 10^5 s) by drawing special attention to the frequency dependence of the dilational storage, $E'(\omega)$, and loss, $E''(\omega)$, moduli of these adsorption layers in the range $\omega \sim 10^{-2}-1$ rad s^{-1}.

Materials and Methods

Initial Chitosan. The chitosan was prepared from Far East crab shells.[25] The degree of acetylation of chitosan was found to be equal to 0.05, and the viscometric-average molar mass was found to be 225 000 from viscometric measurements using the Mark−Houwink relation: $[\eta] = 8.2 \times 10^{-2} \cdot M^{0.76}$.[26] The intrinsic viscosity, $[\eta]$, was determined in the solvent 0.3 M AcOH/0.2 M AcONa; it is found to be equal to 942 mL/g. Then, the overlap concentration, C^*, is admitted in the range of 1 g/L for all of the samples derived from this parent polymer.

Synthesis of Dodecyl Chitosan. The alkylation was performed by a reductive amination reaction as based on our first paper.[11] The conditions adopted are the following: a solution of 10 g of chitosan dissolved in 500 mL of 0.2 M CH_3COOH was added with 350 mL of C_2H_5OH, and the pH was adjusted to 5.05−5.10. Then, 0.496 g of 1-dodecanal was dissolved in 90 mL of C_2H_5OH at 45 °C; the aldehyde solution was added to the chitosan solution under very intensive stirring. Then, reduction is performed with $NaCNBH_3$ before neutralization and isolation of the alkyl chitosans. Under these conditions, the degree of polymerization of the polymers is not modified after the reaction. The polymer has 0.05 as the degree of substitution with a C-12 length of the alkyl chain grafted randomly on the chitosan C-2 position.

NMR Analysis. The acetylation and substitution degrees were determined using ^{1}H NMR. The samples were dissolved in D_2O/HCl at pH ~ 3 and a concentration of 6 mg/mL. ^{1}H NMR experiments were performed using a Bruker DRX400 spectrometer operating at 400 MHz. 1D NMR spectra were collected using 16K data points. Deuterium oxide was obtained from SDS (Vitry, France).

Preparation of Solutions. The polymer solutions are usually prepared at 0.26 g/L of chitosan or hydrophobic chitosan in 0.3 M AcOH; the role of the salt concentration was examined by addition of different amounts of AcONa.

Surface Tension and Dilational Viscoelasticity of Adsorption Layers. A drop tensiometer (Tracker, IT Concept, France) was used to determine the surface tension and its dependence with time by analyzing the axial symmetric shape of a rising air bubble in the aqueous phase (Laplacian profile). The area of a bubble was submitted to periodic, small sinusoidal deformation, allowing continuous measurement of the interfacial tension, γ, and the two-dimensional complex elasticity modulus, $\bar{E}$, of adsorption layers for a sufficiently long time (usually greater than 50 000 s to achieve the quasi-equilibrium state). All measurements were performed at 25 °C.

Practically, this was realized by applying a controlled periodical variation of the drop area, A, according to the sinusoidal law $\bar{\epsilon}(t) = \epsilon_a \exp(i\omega t)$ (where $\bar{\epsilon}(t) = \Delta\bar{A}(t)/A$ is the complex relative dilational deformation of the layer and ϵ_a is the amplitude of this deformation) and by recording the variation of the surface pressure

$$\bar{\pi}(t) = \pi_0 \exp[i(\omega t + \varphi)] \qquad (1)$$

where π_0 is the amplitude of the surface pressure and φ is the phase angle. In the linear deformation regime used in this study, the frequency dependent complex elasticity modulus is defined as

$$\bar{E}(\omega) = d\bar{\pi}/d\bar{\epsilon} = -d\bar{\gamma}/d\bar{\epsilon} = E'(\omega) + iE''(\omega) \qquad (2)$$

TABLE 1: Characteristic Circular Frequencies, ω_{0i}, Elasticity Modules, E_{0i}, and Frequency, ω_c, Corresponding to the Intercept between the Curves $E'(\omega)$ and $E''(\omega)$ for the Adsorption Layers of Chitosan and C_{12}-Chitosan under Different Experimental Conditions (Bulk Polymer Concentration, C_p; Salt Concentration, C_{AcONa})

no.	compound	C_{AcONa} (M)	C_p (g/L)	ω_{01} (rad/s)	E_{01} (mN/m)	ω_{02} (rad/s)	E_{02} (mN/m)	ω_c (rad/s)	τ_c (s)
1	Ch	0	0.26	0.8	60	0.2	9	0.6	10
2	Ch	0.1	3.75	0.045	35.5	0.02	3	0.042	150
3	Ch	1	0.26	0.5	5	0.0025	50	0.0023	2730
4	C_{12}Ch	0	0.26	2	50	0.2	11	1.0	6
5	C_{12}Ch	0.01	0.26	0.3	23	0.01	15	0.011	570
6	C_{12}Ch	0.1	0.26	0.2	3	0.0026	29	0.0025	2510

where the real $E'(\omega)$ and the imaginary $E''(\omega)$ have the meaning of the storage and loss parts by analogy with the 3D rheology.

Inside the limits of the validity of the one relaxation time τ_0 (or one characteristic relaxation frequency, $\omega_0 = 2\pi/\tau_0$) rheological model of Maxwell, the storage and loss moduli could be expressed as

$$E'(\omega) = E_0 \frac{(\omega/\omega_0)^2}{1 + (\omega/\omega_0)^2} \tag{3}$$

$$E''(\omega) = E_0 \frac{\omega/\omega_0}{1 + (\omega/\omega_0)^2} \tag{4}$$

where E_0 is the standard (intrinsic) dilational elasticity modulus which is assumed to be constant in this model as well as the standard (intrinsic) dilational viscosity, $\eta_0 = \tau_0 E_0$. The total dilational elasticity modulus, E, and the phase angle, φ, are defined as

$$E(\omega) = \sqrt{E'^2(\omega) + E''^2(\omega)} = E_0 \frac{\omega/\omega_0}{\sqrt{1 + (\omega/\omega_0)^2}} \tag{5}$$

$$\text{tg}\ \varphi = E''(\omega)/E'(\omega) = \omega_0/\omega \tag{6}$$

It must be pointed out that a one frequency rheological model is valid only for the idealized adsorption layers whose parameters, E_0 and η_0, are constant and independent of the applied frequency, ω. In reality, the constancy of these parameters is disturbed for the adsorption layers of associative polymers, especially hydrophobically modified polymers, which form a physical gel structure by hydrophobic interaction and H-bonding at relatively high concentration. In this case, the parameters E_0 and η_0 become frequency dependent, and the one frequency rheological model of Maxwell becomes insufficient to quantitatively describe the rheological properties of such layers. One of the possible ways to avoid this difficulty is to use a spectrum of characteristic frequencies, ω_{0i}, which allows us by analogy with the 3D rheology[27] to express the two-dimensional moduli as the sums

$$E'(\omega) = \sum_i E_{0i} \frac{(\omega/\omega_{0i})^2}{1 + (\omega/\omega_{0i})^2};\ E''(\omega) = \sum_i E_{0i} \frac{\omega/\omega_{0i}}{1 + (\omega/\omega_{0i})^2} \tag{7}$$

where E_{0i} are the corresponding weights of ith relaxation element to the total elasticity modulus, E_0. Using this procedure, it is possible, in principle, to describe quantitatively all of the details of the rheological behavior of the adsorption layers.

Sometimes, a satisfactory rheological description of the adsorption layers of macromolecules may be realized using only several characteristic frequencies which have a clear physical meaning.[20] Previously,[3,19] it has been assumed that the characteristic relaxation times ~1−10 s and ~10^2−10^3 s relate to different mechanisms which control the dilational viscoelasticity of adsorption layers of surfactants and polymers. The first characteristic relaxation time is usually attributed to the adsorption−desorption exchange of molecules and segments between the surface and the subsurface layer during dilational perturbations,[19] whereas the second time corresponds to slower reconformation of the adsorbed macromolecules inside the adsorption layer.[3,20]

In this paper, we use the two characteristic relaxation times model

$$E'(\omega) = E_{01} \frac{(\omega/\omega_{01})^2}{1 + (\omega/\omega_{01})^2} + E_{02} \frac{(\omega/\omega_{02})^2}{1 + (\omega/\omega_{02})^2} \tag{8}$$

$$E''(\omega) = E_{01} \frac{\omega/\omega_0 1}{1 + (\omega/\omega_0 1)^2} + E_{02} \frac{\omega/\omega_0 2}{1 + (\omega/\omega_0 2)^2} \tag{9}$$

where ω_{0i} and E_{0i} ($i = 1,2$) are characteristic circular frequencies and elasticity moduli, respectively, found by fitting the experimental dependences $E'(\omega)$ and $E''(\omega)$ in the frequency range $\omega = 0.01$−0.1 rad s^{-1}. The crossing frequency, ω_c, corresponding to the intersection of two curves, $E'(\omega)$ and $E''(\omega)$, delimits two characteristic regions: $\omega > \omega_c$ where the adsorption layers behave as solidlike, and $\omega < \omega_c$ relating to liquidlike adsorption layers. It should be pointed out that, in the case when the experimental curves $E'(\omega)$ and $E''(\omega)$ did not intersect in the accessible frequency range $\omega = 0.01$−0.1 rad s^{-1}, the estimation of this crossing frequency, ω_c, has been carried out by the extrapolation of theoretical curves (8) and (9) up to the intersection at some characteristic frequency, ω_c^*. Conventionally, this characteristic frequency, ω_c^*, is considered as coinciding with the crossing frequency, ω_c (see Figure 8b and Table 1).

Results and Discussion

Chitosan (Ch) and dodecyl chitosan (C_{12}Ch) used in this study are cationic polyelectrolytes, in acetic acid, with the same degree of acetylation. The first polysaccharide may be conventionally designed as a nonassociating polyelectrolyte with a few loosely attracting groups (5 mol % −N-acetyl groups). The alkylated chitosan is an amphiphilic polyelectrolyte with a few long alkyl (C_{12}) chains grafted randomly along the chains which are able to interact and form hydrophobic domains in the bulk.[25] The results of the dynamic surface tension and the dilational rheology of monolayers of chitosan (Ch) and dodecyl chitosan (C_{12}Ch) adsorbed from 0.3 M AcOH solutions in the absence and presence of external salt (AcONa) are discussed in the following.

Different Stages of Adsorption of Chitosans. In general, at relatively small bulk polymer concentrations, all of the dynamic surface tension curves, $\gamma(t)$, for the chitosan (Figure 1) as well as for the C_{12}-chitosan (Figure 2) exhibit three more or less pronounced characteristic periods for the adsorption and

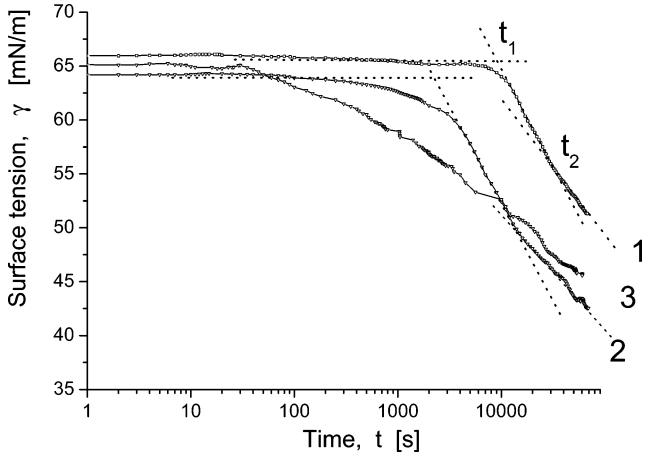

Figure 1. Dynamic surface tension curves, $\gamma(t)$, for the solutions of chitosan at different polymer, C_p (g/L), and salt, C_{AcONa} (M), concentrations: (1) $C_p/C_{AcONa} = 0.26/0$; (2) $C_p/C_{AcONa} = 0.26/1.0$; (3) $C_p/C_{AcONa} = 3.75/0.1$; [AcOH] = 0.3 M, $T = 25$ °C.

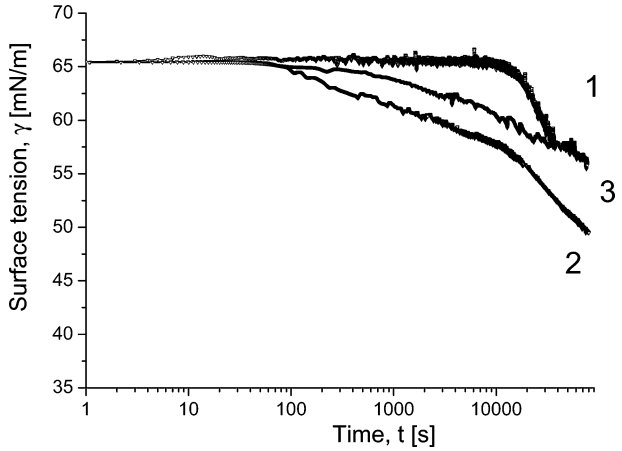

Figure 2. Dynamic surface tension curves, $\gamma(t)$, for the solutions of C_{12}-chitosan ($C_p = 0.26$ g/L) at different salt concentrations, C_{AcONa} (M): (1) $C_p/C_{AcONa} = 0.26/0$; (2) $C_p/C_{AcONa} = 0.26/0.01$; (3) $C_p/C_{AcONa} = 0.26/0.1$; [AcOH] = 0.3 M, $T = 25$ °C.

the formation of the adsorption layers: (1) induction (lag) period, $t < t_1$, corresponding to a very low decrease of the surface tension, γ; (2) post-lag period, $t_1 < t < t_2$, when the rate of the surface tension decrease is maximum; and (3) final period, $t > t_2$, when the surface tension decreases usually with a smaller rate than during the second period.

The lag stage of the adsorption of polymers is controlled by the diffusion rate of macromolecules from the bulk of the solution to the interface. Rather long macromolecules (with $M > 10^5$) adsorb practically irreversibly at the interface because of the large number of hydrophobic groups (N-acetyl and alkyl groups in the case of chitosan and chitosan derivatives) whose immersion in the nonpolar medium leads to considerable gain in the free energy of the system. At this lag stage, the adsorbed macromolecules progressively form rather loose gaseouslike adsorption layers that allow macromolecules to acquire an extended (flat) conformation at the interface (Figure 3, step 1). The new macromolecules which arrive at the interface by diffusion from the bulk of the solution adsorb freely at the interface, and the surface tension is low at this stage of adsorption.

The post-lag period occurs at the time t_1 when the adsorbed macromolecules begin to form dense monolayers and to interact by attractive (molecular and hydrophobic) and by repulsive (steric and electrostatic) forces (Figure 3, step 2). In terms of

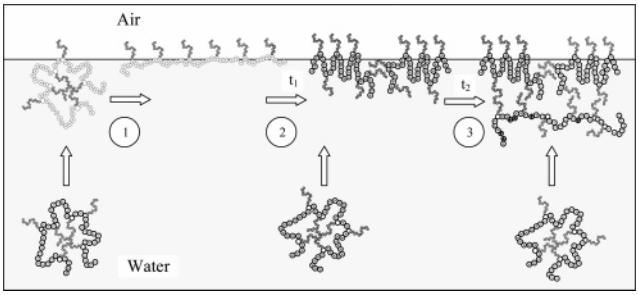

Figure 3. Different stages of formation of the adsorption layer of an alkylated cationic polyelectrolyte during continuous diffusion from the bulk to the interface: (1) coil-to-extended ≪ flat ≫ reconformation during the transfer from gaseous to extended liquid state; (2) transfer form liquid extended to liquid condensed state; (3) formation of the gel-like structure via hydrophobic interaction between alkyl chains of adsorbed and bulk macromolecules.

the thermodynamics of Langmuir monolayers, this corresponds to the transfer from "gaseous" to "liquid extended" state that corresponds to a sharp increase of the surface pressure, $\pi(t) = \gamma_0 - \gamma(t)$, or to the decrease of the surface tension, γ, where γ_0 is the surface tension of the solvent. The slope of the kinetic surface pressure curves, $d\pi/dt$, is maximal at this post-lag stage of adsorption. It has been demonstrated many times[7,16,18,28] that, at this post-lag stage, the adsorption of macromolecules occurs almost freely without spending any considerable work to be introduced inside the adsorption layer.

The effective diffusion coefficient, D_{eff}, of macromolecules estimated according to the relationship[28]

$$\pi(\tau) = \gamma_0 - \gamma(t) \cong RTC_p\sqrt{D_{eff}}\sqrt{t} \qquad (10)$$

is constant for the lag stage of adsorption,[7,18] where C_p is the bulk polymer concentration. Note that eq 10 is derived from the Ward and Tordai equation applicable for the lag time of adsorption[15,17,29]

$$\Gamma(t) = 2C_p\sqrt{D_{eff}t/\pi} \qquad (11)$$

and the simplest equation of state for the gaseous polymeric monolayer, $\pi = \Gamma RT$,[18] where $\Gamma(t)$ is the adsorption amount (mol/m^2) of the polymer at time t and R is the universal gaseous constant. By the way, it has been found[7,18] that the effective diffusion coefficient, D_{eff}, for the macromolecules at this stage of adsorption exceeds by 10^2-10^3 times the "real" diffusion coefficient, D_0, estimated on the basis of the Einstein−Smoluchowski equation, $D_0 = RT/6N_A\pi\eta R_h$,[30] where N_A is the Avogadro number, η is the viscosity of the solvent, and R_h is the hydrodynamic radius of the macromolecule in solution. This high difference between apparent D_{eff} and effective D_0 values has been explained by the multiplicity of adsorbing groups on the adsorbing macromolecule, unlike a small surfactant molecule which brings to the interface only one hydrophobic adsorbing group (for details, see ref 18).

At the end of the post-lag period, t_2, the monolayer becomes saturated by adsorbing segments and exhibits a steric and electrosteric barrier toward newly arriving macromolecules (Figure 3, step 3). The latter must spend much free energy to overpass this energetic barrier to reach the interface by their hydrophobic moieties and to introduce itself inside the adsorption layer. At this post-lag stage, the probability of adsorption of these new macromolecules at the interface ceases to be equal to unity; i.e., the adsorption of macromolecules becomes partially reversible. This is why the rate of adsorption (the slope of the kinetic curve, $\gamma(t)$) of the chitosan) decreases remarkably

during this last stage (Figure 1). On the other hand, with increasing hydrophobicity of macroions, as in the case of HMCh, the newly arriving macromolecules could interact with already adsorbed macroions by forming the second layer. This is typical for the proteins which form structured multilayers,[18,28] and usually leads to some increase of the surface pressure in the time (Figure 2).

Concerning the kinetic curves $\gamma(t)$ for the chitosan obtained at some characteristic values of polymer concentration, C_p, and the ionic strength C_{AcONa} (Figure 1), they do not contradict the general trend found previously for the chitosan samples.[6,7,13,31] Particularly, this concerns the obtained dependence of the lag period t_1 for the formation of adsorption layers on the bulk polymer concentration, C_p, which satisfies the proportionality $t_1 \sim C_p^{-2}$ (the latter follows from the Ward and Tordai adsorption model (eq 2), according to which the product $C_p^2 t_1 = k\Gamma(t_1)/D_{eff}$ is constant, and in which the parameter k is of the order of unity). For example, one finds for the chitosan concentrations 3.75 and 0.26 g/L lag time values of $t_1 \sim 25$ s and $t_1 \sim 10\,000$ s, respectively (curves 1 and 3 in Figure 1). Although this slightly differs from the relationship $t_1 \sim C_p^{-2}$, instead of the expected theoretical value $t_1 \cong 50$ s for the concentration $C_p = 3.75$ g/L (calculated on the basis of the lower polymer concentration), one obtains the experimental value $t_1 \cong 25$ s (curve 3 in Figure 1). Nevertheless, one must conclude for the good correlation between the measured lag times t_1 and those predicted by the Ward and Tordai equation if one takes into account the effect of the salt on t_1.

The effect of the added salt on the lag time of adsorption is more complicated and depends on the nature of polymers, chitosan or C_{12}-chitosan. Although the systematic study of this effect (especially in the region of very low salt concentration) has not been carried out in this paper (these investigations are in progress), one can conclude that the presence of long pending alkyl chains on the macroion backbone influences considerably the kinetics of adsorption and the structure formation inside the adsorption layers. It should be pointed out that, in the absence of the salt, the electrostatic repulsion is strong between both Ch and C_{12}Ch macroions, and their kinetics of adsorption is governed mainly by electrostatic repulsion of adsorbing macroions by already formed adsorption layers. The similarity of lag times, $t_1 \cong 10^4$ s, for Ch and C_{12}Ch (curve 1 in Figures 1 and 2) supports this affirmation.

In general, adding salt decreases the lag time t_1 of adsorption for both Ch and C_{12}Ch, although this decrease is stronger for the latter than for the former. For example, at equal bulk concentrations of polymers, $C_p = 0.26$ g/L, one has $t_1 \cong 2000$ s for the Ch at $C_{AcONa} = 1$ M (curve 2 in Figure 1) and $t_1 \cong 500$ s for the C_{12}Ch at $C_{AcONa} = 0.1$ M (curve 3 in Figure 2). The lag time t_1 for the Ch decreases progressively with the salt concentration from 0 up to 1 M (not shown) (curves 1 and 2 in Figure 1). Surprisingly, at $C_{AcONa} = 0.01$ M, the lag time for the C_{12}Ch decreases down to $t_1 \cong 100$ s and then increases, exhibiting an unexpected behavior explained if one takes into account the different intensities of hydrophobic interactions in both cases which influences the conformation of macroions in the bulk of the solution and at the interface, and their kinetics of adsorption.

In fact, with increasing salt concentration, the electrostatic repulsion between the protonated amino groups decreases. This leads to the decrease of the stiffness of the macroion chain and the degree of swelling that favors the transfer of the macroions from extended coils to a more compact conformation. In the case of chitosan which possesses relatively small nonpolar −N-acetyl and −CH groups, the energy of hydrophobic interaction is relatively low (∼1 kT) and there is no critical transfer from extended to compacted states upon increasing salt concentration. Therefore, one can anticipate that at the interface the chitosan macroion will be mobile and will rapidly acquire an appropriate equilibrium conformation imposed by the concurrence between the energies of adsorption and the intramolecular hydrophobic interactions.

In the case of the C_{12}-chitosan which strongly interacts and adsorbs by its long alkyl chains, the screening of the electrostatic repulsion by adding salt leads to critical aggregation of this associating polyelectrolyte into compact micelle-like aggregates with considerable gain in the free energy (more than 10 kT per one C_{12} chain). Thus, it is not surprising that the adsorption kinetics of the C_{12}-chitosan is much more rapid and the lag times t_1 are systematically less than those for the precursor chitosan (Figures 1 and 2).

We must consider that the Debye−Hückel length, δ_{DH}, which characterizes the electrostatic interaction in polyelectrolyte solutions progressively decreases with the addition of external salt.[32] With increasing C_{AcONa}, this length decreases from $\delta_{DH} \cong 4.5$ nm at $C_{AcONa} = 0$ to $\delta_{DH} \cong 3$ nm at $C_{AcONa} = 10^{-2}$ M (taking into consideration the contribution of the polyelectrolyte and the AcOH). However, when the salt concentration becomes $C_{AcONa} = 10^{-1}$ M, the Debye−Hückel length decreases down to $\delta_{DH} \cong 1$ nm, and for $C_{AcONa} = 1$ M, one has $\delta_{DH} \cong 0.3$ nm. This supports the general rule according to which the almost total screening of the electrostatic repulsion in the polyelectrolyte solutions (the so-called polyelectrolyte effect) is achieved at the electrolyte concentration in the range $C_{AcONa} = 5 \times 10^{-2}-10^{-1}$ M.

Returning to Figure 2, one may try now to rationally explain why the lag time t_1 for the adsorption of the C_{12}Ch decreases non-monotonically with increasing salt concentration in the range $C_{AcONa} = 0-0.1$ M. This lag time decreases from $t_1 \sim 10^4$ s at zero salt concentration to $t_1 \sim 100$ s for $C_{AcONa} = 0.01$ M but is slightly increased to $t_1 \sim 500$ s at $C_{AcONa} = 0.1$ M. One may assume that although the increase of the salt concentration up to $C_{AcONa} = 0.01$ M does not produce the intensive formation of intramolecular aggregates between alkyl chains because of the remaining high electrostatic repulsion (the corresponding Debye−Hückel length is equal to $\delta_{DH} \cong 3$ nm), the repulsion produced by the double layer of adsorbed polyelectrolyte toward the diffusion flow of new arriving macroions to the interface is decreased, leading to some increase of the kinetics of adsorption. Moreover, the macroions are able to spread at the interface with a flat conformation by orienting the maximum of their alkyl chains in contact with the interface. All of these factors lead to the decrease of the lag time (which corresponds to the formation of a saturated monolayer) to the value $t_1 \sim 100$ s (curve 2 in Figure 2).

However, with later increase of the salt concentration up to $C_{AcONa} = 0.1$ M, the Debye−Hückel length decreases down to $\delta_{DH} \cong 1$ nm. Now the electrostatic repulsion between protonated amino groups is practically suppressed, and long alkyl chains are able to form hydrophobic associates with increased free energy higher than 10 kT. This aggregation is enhanced by the hydrophobic attraction between nonpolar −N-acetyl and −CH groups. One can anticipate that the macroions initially adsorb at the interface in the form of these compact aggregates and need some time to acquire the flat conformation at the interface. The driving force of this reconformation is the gain in the free energy of adsorption of long alkyl chains which is slowed down by the intramolecular hydrophobic interactions between alkyl

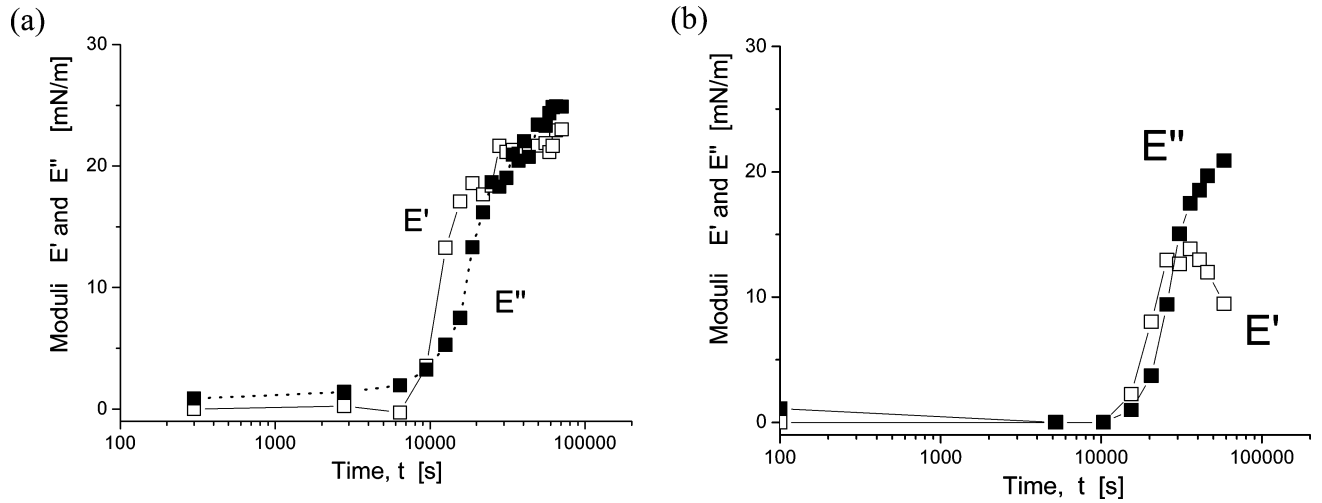

Figure 4. Time dependence of dilational storage, $E'(t)$, and loss, $E''(t)$, moduli at 0.1 Hz for adsorption layers of chitosan (a) and C_{12}-chitosan (b) in the absence of the salt: $C_p = 0.26$ g/M, $C_{AcONa} = 0$, [AcOH] = 0.3 M, $T = 25$ °C.

chains inside the aggregates. Consequently, the lag time of adsorption undergoes some increase to $t_1 \sim 500$ s (curve 3 in Figure 2).

Structure Formation inside the Adsorption Layers of Chitosan and C_{12}-Chitosan in the Absence of Salt. In the course and especially at the end of the post-lag period t_2 of adsorption, the local concentration C_p^s of macromolecules inside the adsorption monolayer begins to highly exceed its bulk value, C_p. Although this local concentration, C_p^s, cannot be determined from the tensiometry, we can expect that its value for strongly adsorbing polymers becomes larger than the bulk overlap concentration (~1 g/L for the C_{12}Ch). At such increased concentration, the macroions are tightly compressed and could sterically interact at the interface and in the water subphase by free (unadsorbed) segments. The attraction between hydrophobic moieties (−N-acetyl and −CH or alkyl groups) of the chitosan and alkylated chitosan derivatives is expected to be due to the spontaneous formation of the physical gel inside the layer of unadsorbed segments, especially with alkylated chitosan.[6,13,20,21]

Kinetics of the Structure Formation. Figure 4 illustrates the increase of both the dilational storage, E', and loss, E'', moduli for chitosan and alkylated chitosan, respectively, at the post-lag and last periods of the formation of adsorption layers. The dilational elasticity moduli were measured at the applied harmonic frequency $\nu = 0.1$ Hz (circular frequency $\omega = 0.63$ rad/s). At this frequency, in the beginning of the post-lag period of formation of the adsorption layers ($t \geq t_1$), both moduli undergo a sharp increase, although the storage modulus, E', is slightly superior to the loss modulus, E''. The approximate equality of the moduli E' and E'' signifies that the applied frequency, ω, is close to the crossing frequency, ω_c, of the adsorption layer, or, in other words, that the Deborah number, $De = \omega/\omega_c$, for these oscillatory rheological tests is approximately equal to unity.[21]

The sharp increase of the dilational storage modulus, E', for the chitosan (Figure 4a) testifies for the intensive formation of reversible (physical) bonds via hydrophobic interaction between N-acetyl and −CH groups. In the case of the alkylated chitosan (Figure 4b), more bulky alkyl chains participate in the formation of hydrophobic bonds. The equality between the moduli E' and E'' signifies that at the applied circular frequency $\omega \sim 0.63$ rad/s, the elastic free energy accumulated in the hydrophobic bonds practically fully dissipates during viscous flow inside the adsorption layer which destroys the gel-like structure formed by these bonds. A slight superiority of the modulus E' with regard to the modulus E'' signifies that at this applied (rather high) frequency some remarkable number of cross-links are not destroyed.

Interestingly, after a long time (t > 30 000 s), the adsorption layers of both chitosan and C_{12}-chitosan undergo a remarkable liquefaction while the loss modulus becomes higher than the storage modulus, $E'' > E'$. The C_{12}-chitosan exhibits even the decrease of the storage modulus, E', whereas that of the chitosan becomes constant. The maximum values E'_{max} for the chitosan and the C_{12}-chitosan are equal to ~22 and 13 mN/m, respectively. This seems unexpected on account of the larger hydrophobicity of the latter with regard to the former. However, we must remember that there is no complete analogy between the 3D and 2D viscoelasticities. In the case of the bulk physical gels, the origin of the storage elasticity is the reversible entropic deformation of macromolecular chains bound by the joints formed by the aggregates of hydrophobic moieties. The loss elasticity is provided from the dissipation of the stored elastic energy upon rupture of the aggregates formed by the hydrophobic groups. In the case of adsorption layers, the dilational viscoelasticity is determined by both the formation of a gel-like structure inside the adsorption layers, on one hand, and adsorption−desorption of alkyl groups at the interface, on the other hand. The storage elasticity of adsorption layers can be realized only if these layers are strongly connected to the interface by a large number of hydrophobic adsorbed groups and if there is no adsorption−desorption of these groups or of the free hydorophobic groups in the neighboring subphase, during the deformation (dilational extension−compression) cycle. Otherwise, relaxation (dissipation) of the stored dilational elasticity accumulated in the form of the excess of the surface tension with regard to its equilibrium state occurs, and the decrease of the dilational storage modulus is observed.

This feature of the two-dimensional dilational viscoelasticity exhibits sometimes unexpected effects. For example, it has been found that the dilational storage modulus, E', of the adsorption layers of an alkylated chitosan decreases with an increase in the bulk concentration, C_p, of this polymer.[13] At low polymer concentration, the adsorbed macromolecules acquire a flat conformation by putting the maximum of their alkyl chains in contact with a nonpolar medium, whereas, at high concentration, the macromolecules adsorb at the interface preferentially in a coiled conformation, and by adsorbing only a part of their alkyl

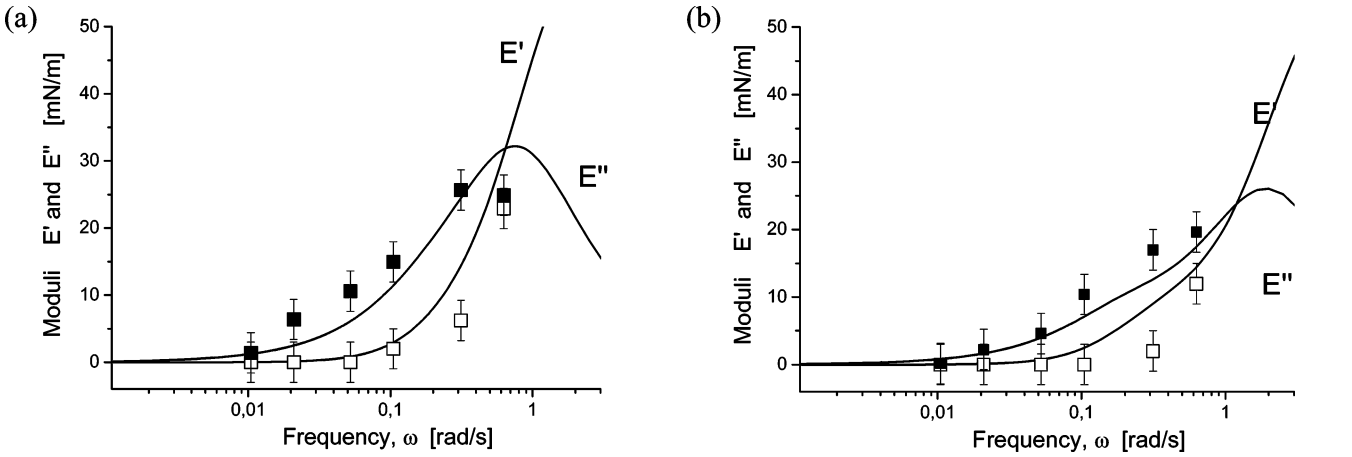

Figure 5. Frequency dependence of dilational storage, $E'(\omega)$ (open squares), and loss, $E''(\omega)$ (filled squares), moduli of adsorption layers of chitosan (a) and C_{12}-chitosan (b) in the absence of the salt: $C_p = 0.26$ g/M, $C_{AcONa} = 0$, [AcOH] = 0.3 M. Lines correspond to the best fitting of the experimental points by the two characteristic relaxation times model (eqs 10 and 11).

chains. In the latter case, during dilational deformation, the free alkyl chains could adsorb at the surface, producing relaxation of the surface tension and consequently the decrease of the elasticity storage modulus, E'. At low bulk polymer concentration, C_p, there is a low concentration of free hydrophobic groups in the vicinity of the surface, and the dilational storage modulus, E', is high and relaxes slowly in time. From Figure 1, the rate of interfacial layer formation is shown to depend strongly on bulk polymer concentration (curves 3 and 1) and evidences the influence of concentration on packing of the polymeric molecules.

By using the above-mentioned argument, we can anticipate that the decrease of the storage modulus, E', after $t > 30\,000$ s (Figure 4b) may be due to the partial desorption of alkyl chains which could form aggregates in the subphase with newly arriving macroions from the solution. Factually, this corresponds to the formation of the gel in the subphasic layer, but the elastic 3D properties of this gel could not be measured by tensiometry. This event can be detected only by the apparent decrease of the dilational storage modulus, E', which testifies for the increasing number of free hydrophobic groups in the neighboring layer. As for the chitosan (Figure 4a), the higher value of the maximal storage modulus, $E'_{max} \cong 22$ mN/m, with regard to the corresponding value, $E'_{max} \cong 13$ mN/m, for the C_{12}Ch at the applied frequency $\omega = 0.63$ rad/s may be explained by the lower energy of adsorption of less hydrophobic N-acetyl groups (for the same rate of diffusion controlled adsorption of free N-acetyl and C_{12} groups, the rate of the relaxation produced by the former is much lower than that for the latter).

Effect of Applied Frequency on the Viscoelasticity of Adsorption Layers. Figure 5 shows how the applied frequency acts on the dilational storage, E', and loss, E'', moduli of adsorption layers of both precursor chitosan and alkylated chitosan in the absence of salt in solution. In the applied circular frequency range $\omega = 0.01-0.63$ rad/s (or the periods $T = 10-600$ s of the sinusoidal oscillations), the adsorption layers of both chitosan and C_{12}-chitosan behave as liquidlike, while $E' < E''$. The hydrophobically modified C_{12}-chitosan is even more "liquidlike", while at the standard frequency $\omega = 0.63$ rad/s its apparent storage modulus, E', is lower than the corresponding modulus, E', of the chitosan.

It has been ascertained that the fitting of experimental curves $E'(\omega)$ and $E''(\omega)$ by the two characteristic frequencies model (eqs 8 and 9) gives always better correlation than the use of the simplest Maxwell model with only one characteristic frequency (eqs 3 and 4). The optimum parameters ω_{0i} and E_{0i}, corresponding to the best fitting of the curves $E'(\omega)$ and $E''(\omega)$ for the chitosan and the C_{12}-chitosan, are presented in Table 1 (lines 1 and 4, respectively). The curves $E'(\omega)$ and $E''(\omega)$ intersect at the characteristic frequencies 0.6 and 1 rad/s, respectively, testifying for the liquidlike behavior of adsorption layers in the whole range of applied frequencies, $\omega = 0.01-0.63$ rad/s. These characteristic frequencies are located in the vicinity of the upper limit, $\omega_{max} = 0.63$ rad/s, of the range of experimentally accessible applied frequencies and thereby could be considered as being equal to corresponding crossing frequencies, ω_c (Table 1). Note that the corresponding crossing times, $\tau_c = 2\pi/\omega_c$, are equal to $\tau_c = 10$ s and $\tau_c = 6$ s for Ch and C_{12}Ch, respectively. The numerical values of two characteristic frequencies, ω_{01} and ω_{02}, are equal to 0.8 and 0.2 rad/s for the Ch and to 2 and 0.2 rad/s for C_{12}Ch. Higher frequency ω_{01} components contribute much more to the intrinsic moduli E_0 compared to lower frequency ω_{02} components, as proved by higher values of the characteristic intrinsic moduli E_{01} with regard to E_{02}.

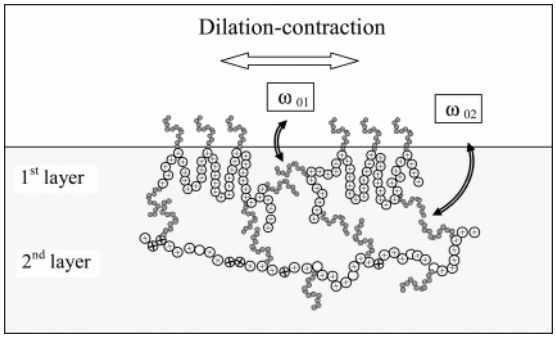

Figure 6. Schematic representation of the relaxation of the surface pressure with different characteristic frequencies (for an explanation, see the text).

First of all, it must be pointed out that the obtained relaxation processes are characterized by relatively low characteristic time in the range of $\tau_r = 3-30$ s. Nevertheless, this time is much larger than the characteristic time, τ_D, for a diffusion that would take free macromolecules or their hydrophobic groups in the course of the exchange between the interface and the interfacial polymeric layer of thickness δ_0 (see Figure 6). This interfacial layer is imagined as being constituted by two parts: (1) the dense adsorption layer in direct contact with the interface by numerous hydrophobic −CH, −N-acetyl, and alkyl groups and

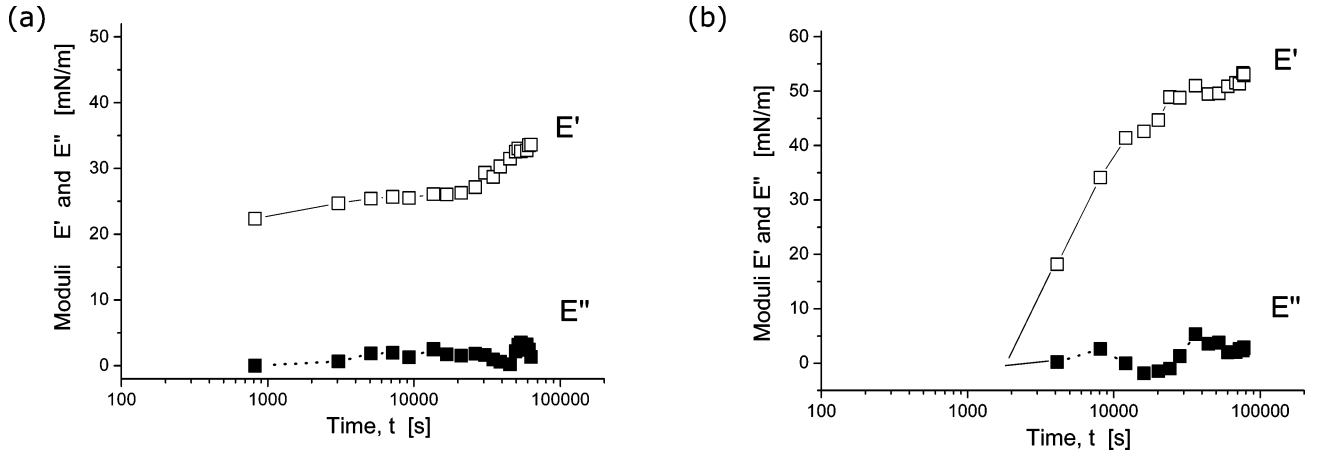

Figure 7. Time dependence of dilational storage, $E'(t)$, and loss, $E''(t)$, moduli of adsorption layers of chitosan ($\omega = 0.63$ rad/s, [AcOH] = 0.3 M, $T = 25$ °C): (a) $C_p = 3.75$ g/M, $C_{AcONa} = 0.1$ M; (b) $C_p = 0.26$ g/M, $C_{AcONa} = 1$ M.

(2) the second gel-like layers formed by the macroions attached to the first layer via hydrophobic interaction between mentioned nonpolar groups. Consequently, the thickness, δ_0, of the interfacial layer is of the order of the size of macromolecular coils, i.e., $\delta_0 \sim 10$ nm. Thus, the characteristic time of diffusion of free (nonbound) hydrophobic groups at this distance may be estimated as $\tau_D \sim \delta_0^2/D_0 \sim 1-10\ \mu$s, where $D_0 \cong 10^{-11}-10^{-10}$ m^2 s^{-1} is the coefficient of diffusion of free segments. In reality, we are not able to observe these very low relaxation times in our oscillatory experiments.

We must admit that the relaxation of the surface pressure with the measured characteristic times of the order of $\tau_r = 3-30$ s occurs via adsorption−desorption of hydrophobic groups which participate in the formation of gel-like structures inside the interfacial layer. Under this assumption, the diffusion of these groups is realized after rupture of hydrophobic bonds with the energy W_a which decreases the effective (apparent) diffusion coefficient

$$D_{eff} = D_0 \exp(-W_a/kT) \qquad (12)$$

Estimating the effective diffusion coefficient as $D_{eff} \sim \delta_0^2/\tau_r \sim 10^{-17}-10^{-16}$ m^2 s^{-1}, one obtains for the activation energy of this thermally activated diffusion the numerical value $W_a = kT \ln(D_0/D_{eff}) \sim 11-14$ kT when $D_0 \sim 10^{-11}$ m^2 s^{-1}. This value has the same order of magnitude as the energy of hydrophobic interaction between two long dodecyl chains or the adsorption energy of this chain at the air/water interface,[5] on one hand, but W_a is somewhat higher than the adsorption or interaction energy between small nonpolar −CH and −N-acetyl groups to which one usually attributes the value ∼1 kT, on the other hand. Nevertheless, we must take into account, that there is always doubt concerning the size of kinetic units (blobs) which participate in this diffusion reptation mechanism. An assumption that this kinetic unit consists of several (two or three D-glucosamine and N-acetyl D-glucosamine) units containing nonpolar −CH or −N-acetyl groups is quite consistent with this activation energy, $W_a = 11-14$ kT, corresponding to the diffusion of the chitosan through the interfacial gel-like layers.

During the dilation cycle, the interfacial area, A, increased by ΔA, and the surface density (the adsorption amount, Γ) of hydrophobic groups in contact with the interface diminishes by $\Delta\Gamma = -\Gamma\epsilon$, where $\epsilon = \Delta A/A$ is the relative deformation of the area. The surface pressure, π, is decreased by $\Delta\pi = -E'\epsilon$, where $E' = \partial\pi/\partial\epsilon$ is the dilational storage modulus, and the thermodynamic equilibrium is disturbed between the interface and the interfacial polymeric layer. This equilibrium is restored by the diffusion of hydrophobic segments from the layer to the interface, and the adsorption of these segments produces the relaxation of the surface pressure (Figure 6). In the case under consideration, the relaxation time is of the order of $\tau_r = 3-30$ s. Inversely, during the contraction cycle, the adsorption amount of hydrophobic groups increased, and these groups tend to leave the interface and diffuse toward and inside the gel-like layer. Obviously, the relaxation of the surface pressure corresponds to the same characteristic relaxation time, $\tau_r = 3-30$ s, because of the similarity between the energies of adsorption and hydrophobic interaction between nonpolar groups of the chitosan.

It must be pointed out that the adsorption layers of chitosan and C_{12}-chitosan in the absence of salt behave similarly. For example, these layers are liquidlike (have relatively low characteristic circular frequencies, ω_{01} and ω_{02}) and are characterized by relatively small ratios of $\omega_{01}/\omega_{02} = 4$ for the former and $\omega_{01}/\omega_{02} = 10$ for the latter (Table 1). This liquidlike behavior is explained by the low degree of hydrophobic aggregation in 0.3 M AcOH aqueous solution where the $-NH_2$ groups of the chitosan and of the C_{12}-chitosan are fully protonated. The electrostatic repulsion between the ionized groups prevents the formation of hydrophobic cross-links between the nonpolar groups and a hard gel-like network formation. In the next paragraph, we will show how the rheological properties of the adsorption layers of chitosan and C_{12}-chitosan are drastically changed upon salt addition.

Effect of the Salt on the Structure Formation inside the Adsorption Layers of Chitosan and C_{12}-Chitosan. Adding salt to 0.3 M AcOH aqueous solutions of chitosan and C_{12}-chitosan produces a systematic shift from liquidlike to solidlike behavior. The effects of the time of formation of polymeric adsorption layers on their dilational elasticity moduli, $E'(t)$ and $E''(t)$, as well as on the frequency dependences of these moduli, $E'(\omega)$ and $E''(\omega)$, are presented in Figures 7−10. The drawn curves in Figures 8 and 10 correspond to the best fitting of the experimental points by the two characteristic relaxation times model (eqs 10 and 11). The fitting parameters for the frequency dependences of these moduli are shown in Table 1.

Comparison between Figures 4a and 5a, on one hand, and Figures 7a and 8a, on the other hand, corresponding to the chitosan adsorption layers, illustrates the drastic changes occurring upon addition of salt to the chitosan solution with a concentration of $C_p = 0.26$ g/L. First of all, it must be pointed out that a considerable increase of the storage modulus, E', and falling down to zero of the loss modulus E'' occurred when the

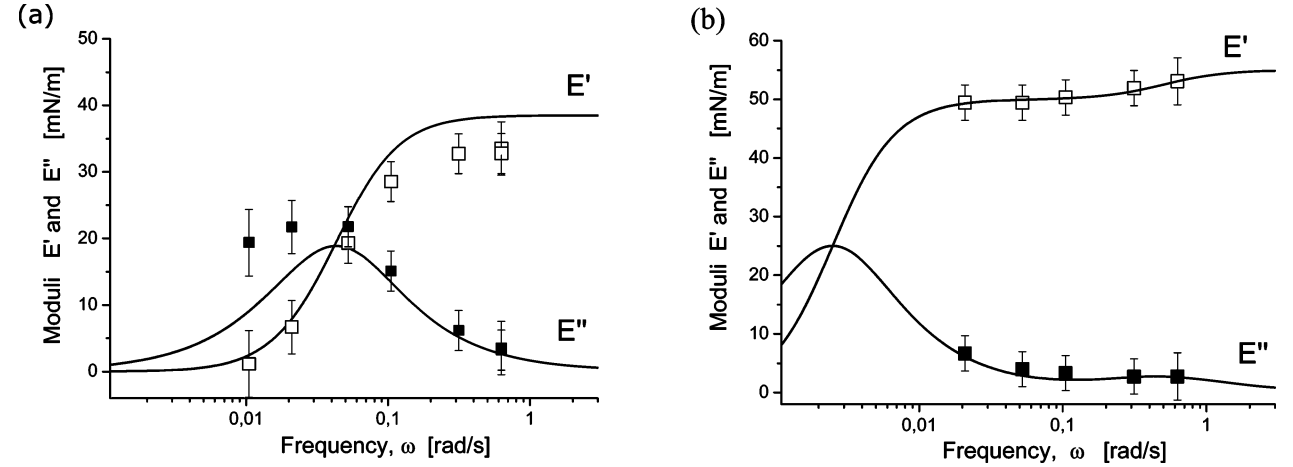

Figure 8. Frequency dependence of dilational storage, $E'(\omega)$, and loss, $E''(\omega)$, moduli of adsorption layers of chitosan ($t_f = 5 \times 10^4$ s, [AcOH] = 0.3 M, $T = 25$ °C): (a) $C_p = 3.75$ g/M, $C_{AcONa} = 0.1$ M; (b) $C_p = 0.26$ g/M, $C_{AcONa} = 1$ M.

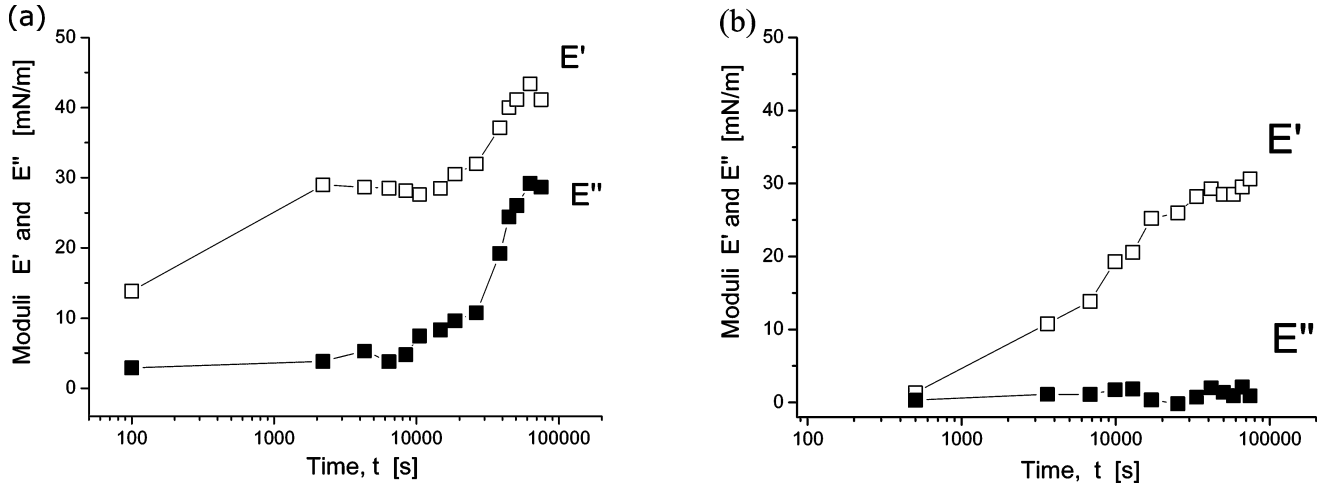

Figure 9. Time dependence of dilational storage, $E'(t)$, and loss, $E''(t)$, moduli of adsorption layers of C_{12}-chitosan ($\omega = 0.63$ rad/s, [AcOH] = 0.3 M, $T = 25$ °C): (a) $C_p = 0.26$ g/M, $C_{AcONa} = 0.01$ M; (b) $C_p = 0.26$ g/M, $C_{AcONa} = 0.1$ M.

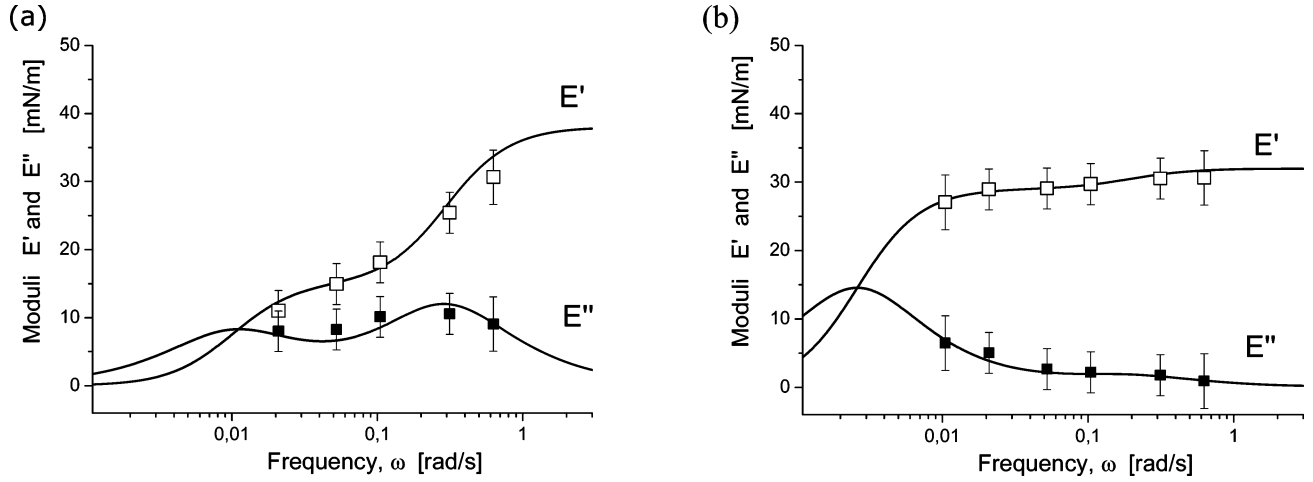

Figure 10. Frequency dependence of dilational storage, $E'(\omega)$, and loss, $E''(\omega)$, moduli of adsorption layers of C_{12}-chitosan ($t_f = 5 \times 10^4$ s, [AcOH] = 0.3 M, $T = 25$ °C): (a) $C_p = 0.26$ g/M, $C_{AcONa} = 0.01$ M; (b) $C_p = 0.26$ g/M, $C_{AcONa} = 0.1$ M.

salt was added (Figures 7a and 8a). At the same time, the frequency, ω_c, that corresponds to the crossing between the theoretical curves $E'(\omega)$ and $E''(\omega)$ is remarkably shifted to the left from $\omega_c \cong 0.6$ rad/s ($\tau_c \cong 10$ s) for zero salt concentration to $\omega_c = 0.0023$ rad/s ($\tau_c = 2730$ s) for $C_{AcONa} = 1$ M (Figures 5a and 8a). It should be pointed out that we conventionally denote this frequency, ω_c, as the crossing frequency (see lines 1 and 3 in Table 1). This represents an obvious illustration of the solidification effect of the salt on the adsorption layers of chitosan. By the way, from Table 1 (lines 1 and 3), it follows that the distance between the characteristic circular frequencies ω_{01} and ω_{02} is remarkably increased upon adding salt. For example, in the absence of the salt, we had $\omega_{01} = 0.8$ rad/s and $\omega_{02} = 0.2$ rad/s, whereas, at $C_{AcONa} = 1$ M, the first frequency

practically does not vary ($\omega_{01} = 0.5$ rad/s), but the second frequency drastically diminishes by 200 times ($\omega_{02} = 0.0025$ rad/s). This splitting of the frequencies is accompanied by the inversion of the contribution of corresponding characteristic moduli, E_{01} and E_{02}, to the resulting viscoelasticity. For example, with increasing salt concentration, the modulus E_{01} decreased from 60 to 5 mN/m, whereas the modulus E_{02} increased from 9 to 50 mN/m. This variation of the characteristic moduli testifies for the transfer of adsorption layers of chitosan from liquidlike to solidlike states upon increasing salt concentration.

It should be noted that, at an intermediate salt concentration, $C_{AcONa} = 0.1$ M (Figure 8a), the frequency $\omega_c = 0.042$ rad/s is situated between two extreme values, $\omega_c = 0.6$ rad/s and $\omega_c = 0.0023$ rad/s, corresponding to $C_{AcONa} = 0$ and $C_{AcONa} = 1$ M, in spite of the increased polymer concentration, $C_p = 3.75$ g/L. The increase of the polymer concentration seems to be responsible for the anomalous decrease of the first characteristic frequency, $\omega_{01} = 0.045$ rad/s (line 2, Table 1), with regard to those corresponding to low chitosan concentration, $C_p = 0.26$ g/L (lines 1 and 3, Table 1). At the same time, the second characteristic frequency, $\omega_{02} = 0.02$ rad/s, seems to obey the decreasing order found for the concentration $C_p = 0.26$ g/L.

In the case of the C_{12}-chitosan (Figures 5b, 9, and 10), the addition of salt produces a similar shift to the left of the frequency, ω_c (see lines 4−6 in Table 1). The numerical value of E_{01} decreases with increasing salt concentration, passing from 50 mN/m ($C_{AcONa} = 10^{-2}$ M) to 3 mN/m ($C_{AcONa} = 0.1$ M). According to the proposed mechanism of the surface pressure relaxation of interfaces bearing adsorption layers of polymers (Figure 6), the value of the first characteristic elasticity modulus, E_{01}, reflects the relative contribution of the fast relaxation with the frequency, ω_{01}, to the total relaxation effect. The decrease of this contribution with increasing salt concentration is related to some solidification of the adsorption layer because of the screening of the electrostatic repulsion between protonated amino groups that favors the formation of the gel-like structure by hydrophobic interaction between long alkyl chains. Gelification decreases the probability of escaping of long alkyl chains from the intermolecular aggregates and their meeting together to form hydrophobic bonds or to adsorb at the interface. Consequently, the relative contribution of the second characteristic elasticity modulus, E_{02}, corresponding to slow relaxation with the frequency ω_{02} gradually increases with increasing salt concentration (see lines 4−6, Table 1).

The formation of the gel-like structure inside the adsorption layer leads to considerable decrease of the local concentration of free (nonbound) segments bearing hydrophobic groups. As a result, this leads to the decrease of the effective diffusion coefficient, $D_{eff} = D_0 \exp(-W_a/kT)$ (eq 12). For example, the relaxation time $\tau_c \sim 1000$ s corresponds to the effective diffusion coefficient $D_{eff} \sim \delta_0^2/\tau_r \sim 10^{-19}$ m^2 s^{-1} related to the interfacial film of thickness $\delta_0 \sim 10$ nm. This corresponds to an activation energy of the diffusion of $W_a = kT \ln(D_0/D_{eff}) \sim 18-19$ kT for $D_0 \sim 10^{-11}$ m^2 s^{-1}.

It is interesting that with increasing electrolyte concentration one observes the pronounced and always increasing split of the characteristic frequencies ω_{01} and ω_{02}: the first frequency, ω_{01}, remains at ∼0.2−0.5 rad/s, whereas the second one, ω_{02}, is sharply depressed down to 10^{-2} rad/s. The former frequency corresponds to the characteristic relaxation time of the order of $\tau_1 \sim 10-30$ /s, as has been found previously in the absence of salt, whereas the second relaxation time increases continuously up to $\tau_1 \sim 2500$ s with increasing salt concentration. At the same time, the corresponding characteristic elasticity moduli E_{01} and E_{02} continuously vary, the former by decreasing and the latter by increasing their absolute values. If one assumes that these different relaxation frequencies, ω_{01} and ω_{02}, correspond to different relaxation mechanisms, one can conclude that the contributions of these mechanisms vary, the former becoming less important and the latter increasing in importance with increasing salt concentration.

One can anticipate that the first mechanism is due to adsorption−desorption of the hydrophobic groups belonging to the first adsorption layer, which is in immediate contact with the interface (Figure 6). The diffusion of these groups takes less time to reach or to leave the interface. The second mechanism is related to diffusion of the hydrophobic segments belonging to the gel-like second layer more distant from the interface. With increasing salt concentration, the relative number of hydrophobic groups near the interface continuously decreases to join the hydrophobic groups of the gel-like layer. Consequently, one observes a continuous transformation of the first mechanism to the second with increasing salt concentration.

Conclusion

The effect of the external salt (AcONa) on the kinetics of adsorption and structure formation inside the adsorption layers of chitosan (Ch) and dodecyl chitosan (C_{12}Ch) as well as on the frequency dependence of the complex dilational elasticity modulus of these layers has been studied.

It has been found that, for both polymers, salt addition results in a decrease of the lag time of adsorption corresponding to the beginning of the formation of a gel-like network inside the adsorption layer via formation of hydrophobic cross-links between nonpolar constitutive −N-acetyl and −CH groups of the Ch or grafted alkyl groups of the C_{12}Ch. This is explained by the screening of the electrostatic repulsion between protonated amino groups of Ch and C_{12}Ch, making the formation of these hydrophobic cross-links and the adsorption of nonpolar groups at the interface easier. In the case of C_{12}Ch, some increase of the lag time has been found for a salt concentration higher than $C_{AcONa} > 10^{-2}$ M, explained by the effect of the self-association (the formation of micelle-like aggregates) between long alkyl chains on their adsorption kinetics.

It has been found that salt addition produces a remarkable effect on the solidification of adsorption layers for Ch and C_{12}Ch. In the absence of salt, at the applied standard frequency $\omega = 0.63$ rad/s, the dilational storage modulus, E', is lower that the loss modulus, E'', testifying for the liquidlike behavior, whereas, at $C_{AcONa} > 0.1$ M, one has always $E' \gg E''$, corresponding to a solidlike behavior of adsorption layers. The frequency scanning of the dilational viscoelasticity of adsorption layers of both polymers in the range $\omega = 0.01-0.63$ rad/s has shown that the frequency, ω_c, corresponding to the intercept between storage, $E'(\omega)$, and loss, $E''(\omega)$, elasticity moduli curves, gradually varies from $\omega_c > 1$ rad/s to $\omega_c < 0.01$ rad/s when the salt concentration increased from zero to $C_{AcONa} = 1$ M. It has been found that C_{12}Ch, having long grafted alkyl chains, exhibited a higher sensitivity to the presence of salt than Ch: the former solidifies more readily and at lower salt concentrations than the latter.

It has been found that the simple rheological model of Maxwell corresponding to only one characteristic relaxation time, τ_0 (or one relaxation frequency, ω_0), is never convenient to correctly describe the frequency dependence of elasticity moduli $E'(\omega)$ and $E''(\omega)$ for the adsorption layers of Ch and C_{12}Ch, especially at increased salt concentrations. The best description has been achieved in all cases when a two relaxation

times model was applied with the characteristic frequencies ω_{01} and ω_{02} being equal to ~ 1 and $\sim 10^{-3}-10^{-2}$ rad/s, respectively. It has been supposed that a higher frequency, ω_{01}, corresponds to the relaxation of the surface pressure by adsorption−desorption of hydrophobic fragments belonging to macroions in the adsorption layer located in the vicinity of the interface. The lowest frequency, ω_{02}, is related to the dissociation of more distant hydrophobic fragments forming cross-links and their diffusion by a reptation mechanism across the dense adsorption layer toward the interface. The corresponding components of the characteristic elasticity moduli E_{01} and E_{02} gradually vary with the addition of salt, the former by decreasing and the latter by increasing their absolute values.

Acknowledgment. V.G.B. thanks Joseph Fourier University in Grenoble (France) for his associate professor position and CNRS-CERMAV.

References and Notes

(1) Sinquin, A.; Houzelle, M. C.; Hubert, P.; Choplin, L.; Viriot, M. L.; Dellacherie, E. *Langmuir* **1996**, *12*, 3779.

(2) Babak, V. G.; Rinaudo, M.; Desbrieres, J.; Vikhoreva, G. A.; Michalski, M.-C. *Mendeleev Commun.* **1997**, *4*, 149.

(3) Millet, F.; Nedyalkov, M.; Renard, B.; Perrin, P.; Lafuma, F.; Benattar, J.-J. *Langmuir* **1999**, *15*, 2112.

(4) Babak, V. G.; Skotnikova, E. A.; Lukina, I. G.; Pelletier, S.; Hubert, P.; Dellacherie, E. *J. Colloid Interface Sci.* **2000**, *225*, 505.

(5) Tanford, C. *The Hydrophobic Effect, Formation of Micelles and Biological Membranes*, 2nd ed.; Wiley: New York, 1980.

(6) Babak, V.; Desbrieres, J. *Colloid Polym. Sci.* **2006**, *284*, 745.

(7) Babak, V. G.; Desbrieres, J. *Mendeleev Commun.* **2004**, *2*, 66.

(8) Babak, V. G.; Tikhonov, V. E.; Lachashvili, A. R.; Philippova, O. E.; Khokhlov, A. R.; Rinaudo, M. *Mendeleev Commun.* **2003**, *5*, 217.

(9) Philippova, O. E.; Volkov, E. V.; Sitnikova, N. L.; Khokhlov, A. R.; Desbrieres, J.; Rinaudo, M. *Biomacromolecules* **2001**, *2*, 483.

(10) Babak, V. G.; Auzely, R.; Rinaudo, M.; Khokhlov, A. R. *Mendeleev Commun.* **2005**, *15*, 239.

(11) Desbrieres, J.; Martinez, C.; Rinaudo, M. *Int. J. Biol. Macromol.* **1996**, *19*, 21.

(12) Babak, V. G.; Lukina, I. G.; Vikhoreva, G. A.; Desbriere, J.; Rinaudo, M. *Colloids Surf., A* **1999**, *147*, 139.

(13) Babak, V. G.; Desbrieres, J.; Tikhonov, V. E. *Colloids Surf., A* **2005**, *255*, 119.

(14) Ercelen, S.; Zhang, X.; Duportail, G.; Grandfils, C.; Desbrieres, J.; Karaeva, S.; Tikhonov, V.; Mely, Y.; Babak, V. *Colloids Surf., B* **2006**, *51*, 140.

(15) Hansen, F. K.; Myrvold, R. *J. Colloid Interface Sci.* 1**995**, *176*, 408.

(16) Beverung, C. J.; Radke.C. J.; Blanch, H. W. *Biophys. Chem.* **1999**, *81*, 59.

(17) Miller, R.; Fainerman, V. B.; Aksenenko, E. V.; Leser, E;, M.; Michel, M. *Langmuir* **2004**, *20*, 771.

(18) Babak, V. G.; Boury, F. *Colloids Surf., A* **2004**, *243*, 33.

(19) Saulnier, P.; Boury, F.; Malzert, A.; Heurtault, B.; Ivanova, T.; Cagna, A.; Panaiotov, I.; Proust, J. E. *Langmuir* **2001**, *17*, 8104.

(20) Babak, V. G.; Desbrieres, J. *Mendeleev Commun.* **2005**, *1*, 35.

(21) Babak, V.; Desbrieres, J. *Mendeleev Commun.* **2005**, *5*, 190.

(22) Babak, V.; Auzely, R.; Khokhlov, A.; Rinaudo, M. Interfacial Layer-by-Layer Interpolyelectrolyte and Surfactant/Polyelectrolyte Complex Formation Studied by Flow Dilational Rheometry; 4th World Congres on Emulsions, Lyon, France, 2006.

(23) Babak, V. G. Colloid properties of derivatives of chitin and chitosan. Theory and practical application. In *Chitin and chitosan. Production, Properties and Usage*; Skryabin, K. G., G. A. V., Varlamov, V. P., Eds.; Nauka: Moscow, 2003; p 201.

(24) Rinaudo, M. *Prog. Polym. Sci.* **2006**, *31*, 603−632.

(25) Rinaudo, M.; Auzely, R.; Vallin, C.; Mullagaliev, I. *Biomacromolecules* **2005**, *6*, 2396.

(26) Brugnerotto, J.; Desbrières, J.; Roberts, G.; Rinaudo, M. *Polymer* **2001**, *42*, 9921.

(27) Wee, W.-K.; Mackley, M. R. *Chem. Eng. Sci.* **1998**, *53*, 1131.

(28) Eastoe, J.; Dalton, J. S. *Adv. Colloid Interface Sci.* **2000**, *85*, 103.

(29) Ward, A. F. H.; Tordai, L. *J. Chem. Phys.* **1946**, *14*, 453.

(30) Hiemenz, P. C. *Principles of Colloids and Surface Chemistry*, 2nd ed.; Marcel Dekker: New York, 1986.

(31) Desbrieres, J.; Babak, V. G. *Polym. Int.* **2006**, *55*, 1177.

(32) Malovikova, A.; Milas, M.; Rinaudo, M.; Borsali, R. In *Macroion characterization from dilute solutions to complex fluids*; Schmitz, K. S., Ed.; ACS Symposium Series, Vol. 548; American Chemical Society: Washington, DC, 1994; p 315.